Shallow energy levels around solitons, polarons and bipolarons in quasi-one-dimensional MX compounds



1999 J. Phys.: Condens. Matter 11 4647

(http://iopscience.iop.org/0953-8984/11/24/306)

J. Phys.: Condens. Matter **11** (1999) 4647–4656. Printed in the UK PII: S0953-8984(99)00810-3

# Shallow energy levels around solitons, polarons and bipolarons in quasi-one-dimensional MX compounds

J H Wei, D S Liu, S J Xie and L M Mei

Department of Physics, Shandong University, Jinan, Shandong, 250100, People's Republic of China

Received 6 January 1999, in final form 17 March 1999

**Abstract.** Shallow energy levels in quasi-one-dimensional MX compounds have been found firstly by considering the two-band tight-binding model. These shallow levels are situated at the band edges of the CB and VB. The electronic states of the shallow levels are localized around solitons, polarons and bipolarons. It is expected that these shallow levels could be observed in the absorption spectrum of MX compounds. Finally, the effect of e–e interactions on the shallow levels was studied. It has been found that e–e interactions will decrease the mini-gap between the shallow levels and CB and increase the mini-gap between the shallow levels and VB.

## 1. Introduction

Halogen-bridged transition-metal complexes (so-called MX chains) exhibit low dimensionality, mixed valence, strong electron–phonon (e–ph) and electron–electron (e–e) interactions [1–5]. They have alternating transition-metal (M = Ni, Pd or Pt) and halogen (X = Cl, Br or I) atoms in chains, which are aligned parallel to each other and surrounded by various types of ligand structure L (L = X, ethylamine, ethylenediamine, cyclohexanediamine etc). MX compounds can be easily tuned by chemical variation of M and X, by pressure or by doping [6, 7], which makes MX chains useful model systems for testing theories of one-dimensional (1D) solids especially the competition between e–e and e–ph interactions. The structure of a PtCl chain is shown in figure 1. Therefore it has been attracting much attention both in experimental [8–12] and theoretical area [13–18] in recent years.

The electronic structure of MX compounds is composed of the half-filled $d_{z^2}$ orbitals of metals, and the filled $p_z$ orbitals of halogens. In complexes with M = Pt or Pd, the energy level of the $p_z$ orbital of halogens is much lower than that of the $d_{z^2}$ orbital of metals [19]. Bishop, Gammel and Phillpot employed a two-band model to describe the electronic energy levels of PtX (X = Cl, Br, I) [13, 14]. It was found that the ground state is twofold degenerate. Solitons, polarons and bipolarons can be excited as stable excitations in MX chains. For the ground state, the lattice structure is dimerizational for the X sub-lattice, accompanied by a charge density wave (CDW) of the M sub-lattice. The $4a$ period results in the electronic energy band splitting into four sub-bands. The lower two filled sub-bands correspond to the X majority bands and the upper two to those of the metal. The top M sub-band is empty and the lower one is filled. So the system is three-quarters filled.

Solitons, polarons and bipolarons are localized excitations in the MX chain, which result in deep energy levels in the forbidden bands. The electronic states corresponding to these deep energy levels are localized around the excitations. In the soliton case, two deep energy

0953-8984/99/244647+10$19.50  

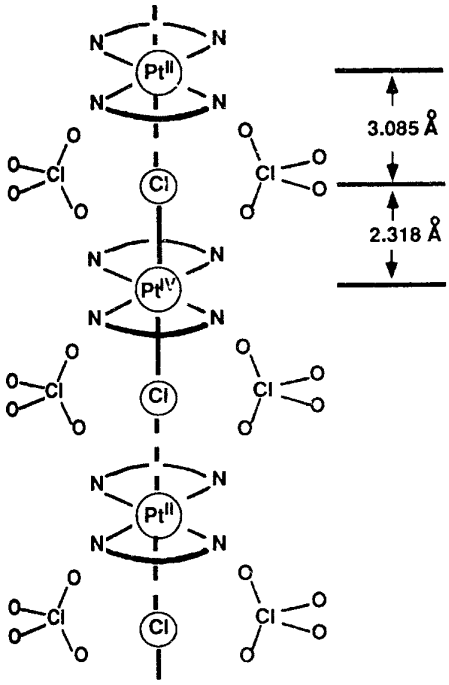


**Figure 1.** Structure of the PtX material, $[Pt(en)_2][Pt(en)_2Cl_2](ClO_4)_4$.

levels were found, one in the forbidden band of the X sub-bands, another in the forbidden band of the M sub-bands. In the polaron or bipolaron case, four deep energy levels were found, two in the forbidden band of the X sub-bands, others in the forbidden band of the M sub-bands [13]. The reason for forming these localized states is simple. Since the soliton, for example, is a domain wall between two degenerate dimerization phases, there appears lattice deformation in the soliton area. Such deformation potential can trap the electrons or holes to form some bound states, which are localized around the soliton. In one-dimensional conducting polymers, it was reported that besides the deep energy levels, shallow energy levels will also emerge out from the band edges if one adopts the Su–Schrieffer–Heeger (SSH) model instead of the Takayama–Linliu–Maki (TLM) model [20, 21]. The TLM model is a continuum approximation of the SSH model in the limit of weak coupling, and such an approximation loses some localized states. The appearance of the shallow energy levels results from the strong e–ph coupling. The e–ph coupling in MX compounds is suggested to be stronger than that in conducting polymers, so shallow energy levels in MX compounds will be expected. In this paper, we employed the two-band extended Peierls–Hubbard model [13, 14] with a more accurate method and more careful calculation. In section 2, the model Hamiltonian is described and we then outline briefly the scheme of a self-consistent calculation. In section 3, theoretical calculations are presented for PtCl, PtBr and PtI. The electronic states are investigated, and the properties of electronic states around solitons, polarons and bipolarons are discussed. Finally, in section 4, some conclusions are summarized.

## 2. Model and calculation

Many previous tight-binding models for MX compounds have been assumed by considering a single orbital on metal atoms and electron transfer for the nearest neighbouring orbitals in

one chain. The electron–lattice interaction is caused by displacements of the halogen atoms, which give fluctuation of the electron potential at the metal sites. The role of electron–electron interactions is considered in the Hubbard model. Of all the models, the two-band extended Peierls–Hubbard model is a significant one, which reads

$$H = \sum_{n,s}[-t_0 + \alpha(u_{n+1} - u_n)](C^+_{n,s}C_{n+1,s} + \text{HC}) + \sum_{n,s}[(-1)^n e_0 - \beta(u_{n+1} - u_{n-1})]C^+_{n,s}C_{n+1,s} + \frac{k_{MX}}{2}\sum_n (u_{n+1} - u_n)^2 + \frac{U}{2}\sum_{n,s} C^+_{n,s}C_{n,s}C^+_{n,-s}C_{n,-s} \tag{1}$$

where $t_0$ is the electron hopping integral in a uniform lattice spacing, $\alpha$ and $\beta$ ($= \beta_M, \beta_X$) the inter-site and on-site e–ph coupling constant, $2e_0$ the difference between metal and halogen electron affinities. $C^+_{n,s}$ ($C_{n,s}$) denotes the creation (annihilation) operator for the electronic orbital at the $n$th atom with spin $s$, whereas $u_n$ is the displacement from uniform lattice spacing of the atom at site $n$, $k_{MX}$ is the stiffness constant and $U$ is the Hubbard parameter of the e–e interaction.

With a small deviation from the equilibrium configuration $\{u_n\}$, the static condition can be derived by minimizing the total energy of the system through the perturbation theory, which gives

$$u_n = \frac{1}{2}(u_{n+1} + u_{n-1}) - \frac{\alpha}{k_{MX}}{\sum_{\mu,s}}' Z_{n,\mu,s}(Z_{n-1,\mu,s} - Z_{n+1,\mu,s}) + \frac{\beta_{n+1}}{2k_{MX}}{\sum_{\mu,s}}' Z_{n+1,\mu,s}Z_{n+1,\mu,s} + Z_{n-1,\mu,s}Z_{n-1,\mu,s}. \tag{2}$$

Here, prime means summarization for the occupied states. A periodic boundary condition was imposed,

$$Z_{N+1,\mu,s} = Z_{1,\mu,s} \qquad u_{N+1} = u_1.$$

The electron wavefunction is given in the Wannier orbital $|n\rangle$ by

$$|\Psi_{\mu,s}\rangle = \sum_n Z_{n,\mu,s}|n\rangle.$$

Therefore, $|Z_{n,\mu,s}|^2$ denotes the probability of electron eigenstate $\mu$ on site $n$. $Z_{n,\mu,s}$ and the corresponding eigenvalue $\varepsilon_{\mu,s}$ are determined by the following eigenequation,

$$[-t_0 + \alpha(u_{n+1} - u_n)]Z_{n+1,\mu,s} + [-t_0 + \alpha(u_n - u_{n-1})]Z_{n-1,\mu,s} + [(-1)^n e_0 - \beta_n(u_{n+1} - u_{n-1})]Z_{n,\mu,s} + U\langle C^+_{n,-s}C_{n,-s}\rangle Z_{n,\mu,s} = \varepsilon_\mu Z_{n,\mu,s}. \tag{3}$$

The e–e interaction term was simply treated in the unrestricted Hartree–Fock approximation.

To estimate the localization of the electronic states, we introduce localized factor $I_{\mu,s}$,

$$I_{\mu,s} = \sum_{n=1}^{N} |Z_{n,\mu,s}|^4. \tag{4}$$

For a completed extended state, $Z_{n,\mu,s} = 1/\sqrt{N}$ approximately for each $n$, $I_{\mu,s} = 1/N \to 0$ ($N \to \infty$), while for a completed localized state, $Z_{n,u,s} = \delta_{n,n_0}$ (namely an electron is localized only in site $n_0$), $I_{\mu,s} = 1$. In general, we have $0 \leqslant I_{\mu,s} \leqslant 1$. So the value of $I_{\mu,s}$ indicates the localized degree of electronic states.

Equations (2) and (3) are solved numerically for an MX chain with a total number $N$ of atoms by means of a self-consistent iterative method. When the change of $u_n$ (in units of Å) is less than $10^{-6}$ or of the total energy less than $10^{-12}$ for two successive iterations, the iteration process stops.

## 3. Calculation and discussion

We make calculations on PtCl, PtBr and PtI compounds. The parameters (listed in table 1) for these materials have been suggested from the band structure calculation [22] and the valence-bond calculations on small clusters [23], which have been optimized to match the ground-state experimental data. These numbers are to be interpreted as effective $U = 0$ mean-field values.

**Table 1.** Parameters for PtX (X = Cl, Br, I) compounds.

| | $t_0$ (eV) | $\alpha$ (eV Å$^{-1}$) | $E_0$ (eV) | $\beta_M$ (eV Å$^{-1}$) | $k_{MX}$ (eV Å$^{-2}$) |
|---|---|---|---|---|---|
| PtCl | 1.54 | 2.38 | 0.924 | 0.160 | 3.91 |
| PtBr | 1.30 | 2.17 | 0.520 | 0.512 | 5.03 |
| PtI | 1.99 | 2.65 | 0.398 | 0.212 | 7.19 |

**Table 2.** Experimental data and theoretical results of PtX compounds.

| | $\Delta$ (Å) | | $E_g$ (eV) | | $A$ (eV) | | $B$ (eV) | | $C$ (eV) | |
|---|---|---|---|---|---|---|---|---|---|---|
| | Cal | Exp | Cal | Exp | Cal | Exp | Cal | Exp | Cal | Exp |
| PtCl | 0.38 | 0.38 | 2.5 | 2.5 | 1.53 | 1.68 | 2.1 | 2.0 | 0.6 | 0.4 |
| PtBr | 0.24 | 0.24 | 1.5 | 1.5 | 0.3 | 0.49 | 0.8 | 0.84 | 1.05 | 1.08 |
| PtI | 0.15 | 0.15 | 1.2 | 1.2 | 0.3 | 0.43 | 0.63 | 0.66 | 0.85 | 0.83 |

The ground state of PtCl has a lattice structure of dimerization for the X sub-lattice, accompanied by a charge density wave (CDW) of the Pt sub-lattice. When the charge-transfer (CT) band of PtCl is excited, it was found that new three main absorption bands appear below the CT band gap $E_g$, called A (1.68 eV), B (2.0 eV) and C (0.4 eV) [26, 27], which were assigned to the polaron excitations. Similar phenomena have been observed in PtBr [28] and PtI [29]. The experimental data and our calculated results are listed in table 2.

It was found that our calculations reproduce the observed lattice distortion amplitude ($\Delta$), optical gap ($E_g$) [24, 25] and the transition absorption of excitations. This confirms the correctness of the two-band model used here to describe the quasi-one-dimensional PtX compounds. It should be pointed out that in PtBr or PtI, bands A and C originate from polarons while band B from solitons.

We calculated the band gap $E_g$ with different numbers $N$ for the chain in a periodic boundary condition. The result is shown in figure 2. It can be seen that, for PtI, when the chain consists of 24 atoms or less, the band gap increases with decreasing of the chain length. As well known, periodic boundary conditions will be not suitable to describe a short chain. In this case, boundaries of a system may play an important role. So a natural or end-fixed boundary condition may be more suitable for a short-chain system [30]. To dismiss the problem of boundary condition, we took $N \geqslant 120$, which corresponds to a fairly long chain in the calculation.

The energy levels of solitons are shown in figure 3(a). Two deep energy levels were obtained, which are known as the soliton levels. In addition, four shallow levels are found in PtCl, two of which, designed c1 and c2, emerge from the bottom of the conduction band and the other two, designed v1 and v2, from the top of the lowest valence band. The mini-gap between c1 (c2) and the conduction band is 0.05 eV (0.03 eV). The wavefunctions of shallow

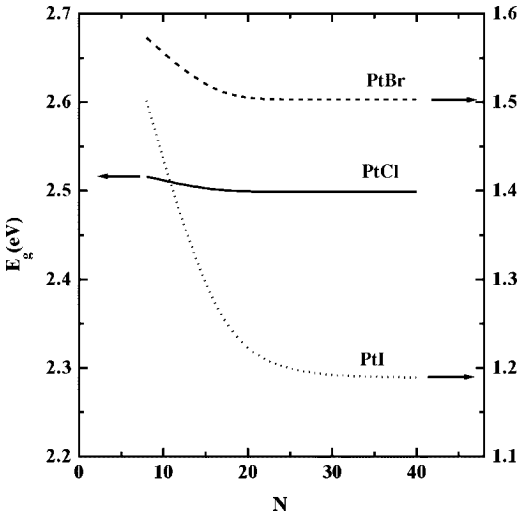


**Figure 2.** Dependence of the band gap $E_g$ on chain lengths in the periodic boundary condition.

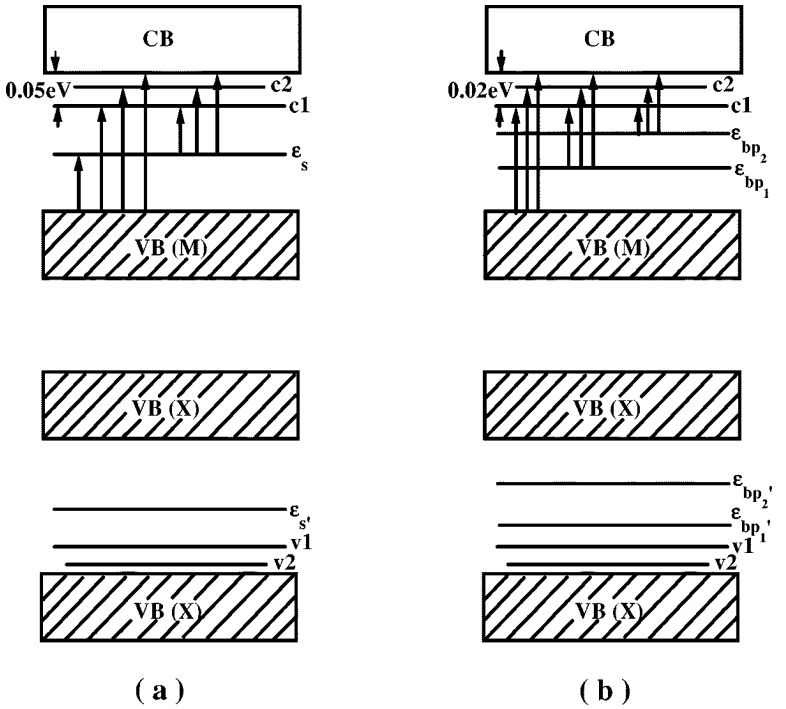


**Figure 3.** Energy spectra of neutral soliton (a) and charged bipolaron (b) in PtCl.

and deep levels are plotted in figure 4. As expected, the wavefunctions of the shallow levels are apparently localized around the soliton. The localized factors and parities of the wavefunctions are shown in table 3.

From table 3, we see that wavefunctions of the deep levels both have even parities. Wavefunctions of shallow levels c1 and v1 have odd parities, while functions of shallow

**Table 3.** The parities and factors of localized energy levels in the soliton case.

| | v2 Even | v1 Odd | $\varepsilon_s'$ Even | $\varepsilon_s$ Even | c1 Odd | c2 Even |
|---|---|---|---|---|---|---|
| PtCl | 0.088 | 0.129 | 0.425 | 0.290 | 0.194 | 0.166 |
| PtBr | — | 0.068 | 0.260 | 0.206 | 0.113 | — |
| PtI | — | — | 0.108 | 0.097 | — | — |

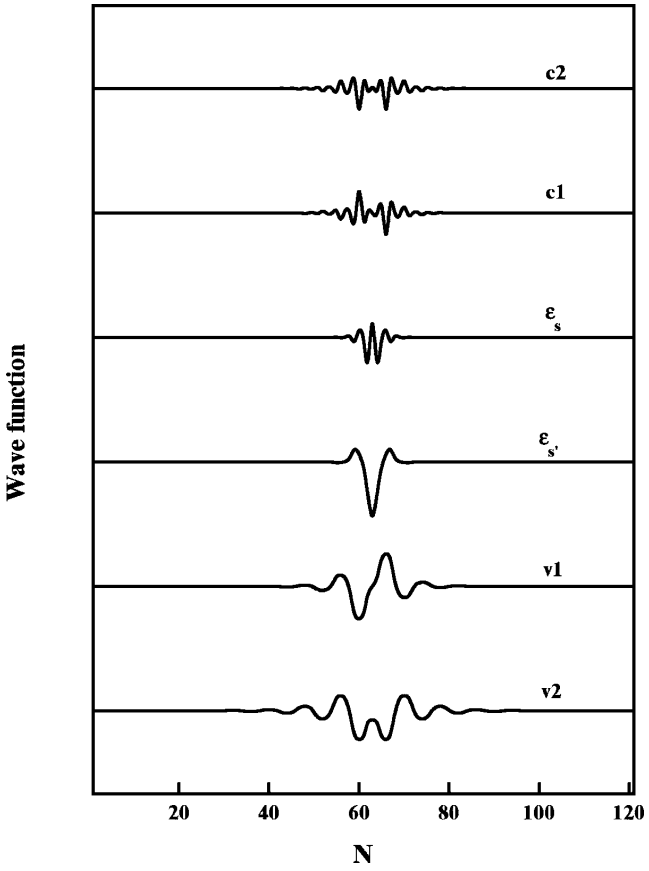


**Figure 4.** Localized wavefunctions of shallow and deep energy levels of a soliton in PtCl.

levels c2 and v2 even. The localization of levels c1 and c2 is stronger than that of v1 and v2. In PtBr, two shallow levels (c1 and v1) were found, while in PtI, only deep levels were obtained, no shallow levels being found. The localization of the shallow energy levels becomes weak from PtCl to PtI.

For a polaron state, four deep levels were obtained, which are known as polaron levels. It was found that only one shallow level under the bottom of the CB emerges in PtBr. This shallow level shifts down 0.01 eV from the band edge of the CB. In PtCl and PtI, no shallow levels were found.

For a bipolaron state, four deep levels were obtained, which are known as bipolaron levels. In addition, four shallow energy levels were found in PtCl, which are designed c1, c2, v1 and v2 as shown in figure 3(b). The mini-gap between c1 (c2) and conduction band is 0.02 eV

**Table 4.** The parities and factors of localized energy levels in the bipolaron case.

| | v2 Even | v1 Odd | $\varepsilon'_{bp_1}$ Even | $\varepsilon'_{bp_2}$ Odd | $\varepsilon_{bp_1}$ Odd | $\varepsilon_{bp_2}$ Even | c1 Odd | c2 Even |
|---|---|---|---|---|---|---|---|---|
| PtCl | 0.044 | 0.073 | 0.253 | 0.245 | 0.282 | 0.261 | 0.144 | 0.126 |
| PtBr | — | 0.090 | 0.141 | 0.136 | 0.115 | 0.131 | 0.150 | — |
| PtI | — | 0.025 | 0.056 | 0.056 | 0.052 | 0.053 | 0.037 | — |

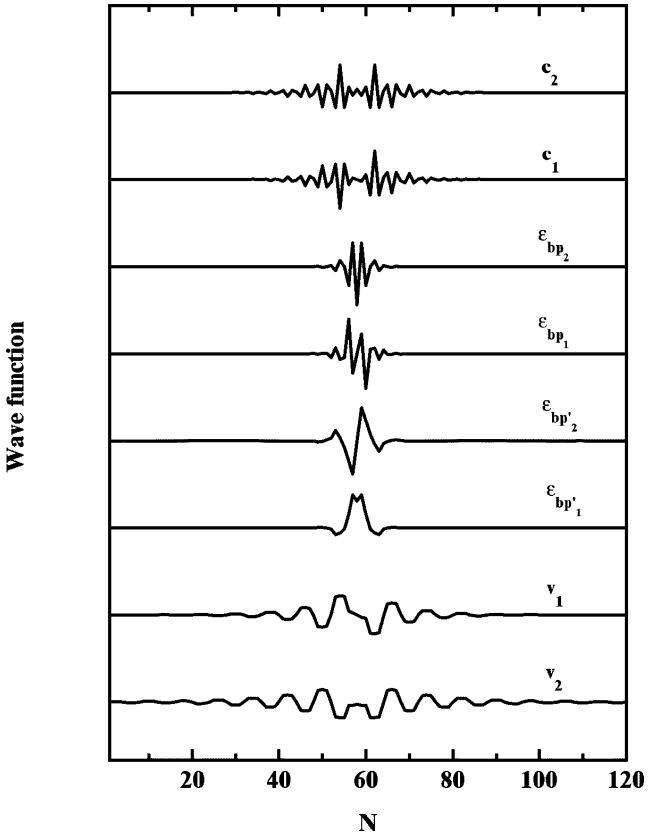


**Figure 5.** Localized wavefunctions of shallow and deep energy levels of a bipolaron in PtCl.

(0.015 eV). The properties of the localized levels are listed in table 4. The corresponding wavefunctions are shown in figure 5. We see that wavefunction c1 or v1 has an odd parity, while c2 or v2 has an even parity. Similar to the soliton case, the localization of level c1 (c2) is stronger than that of v1 (v2). In PtBr and PtI, two shallow levels (c1 and v1) were found. It was found that, although the localization of deep levels becomes weak from PtCl to PtI, the localization of the shallow energy level c1 and v1 is strongest in PtBr.

Based on the above results, we can theoretically give a schematic absorption spectrum for the solitons, polarons and bipolarons. As shown in figure 3(a), in the neutral soliton case, for example, three group transitions were expected; the first one corresponds to the transition from VB to the soliton level, the second one from VB to CB and the last one from the soliton level to CB. Due to the existence of the shallow level c1 (c2), the latter two groups of transitions will result in a shoulder in the corresponding absorption spectrum.

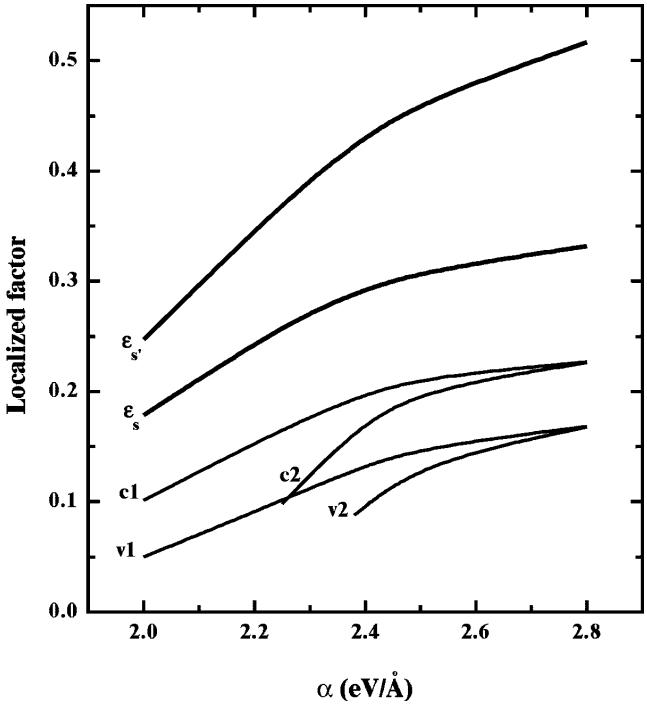


**Figure 6.** Dependence of the localization factors of shallow and deep energy levels of a soliton on the e–ph coupling constant $\alpha$ in PtCl. The wide lines represent the deep levels and the narrow lines the shallow ones.

The emergence of shallow energy levels is the result of excitations. The numbers and degrees of localization of shallow levels vary with materials. In the following, the effect of the e–ph coupling parameter $\alpha$ was studied. As shown in figure 6, with increasing e–ph coupling $\alpha$, the localization of both the deep levels and the shallow levels of solitons increases. In the limit of weak coupling ($\alpha < 2.0$ eV Å$^{-1}$), although the deep levels still exist, it was found that the shallow levels merge into the bands and the corresponding wavefunctions become extended, while c2 and v2 will vanish at a larger e–ph coupling. The effect of e–ph coupling $\alpha$ on the localized levels of bipolarons is shown in figure 7. For the deep levels, the localization increases with increasing $\alpha$. The increase becomes apparent in the range of middle intensity of e–ph coupling. For the shallow levels, a strange phenomenon was obtained for c1 and v1. The localization of c1 and v1 does not increase monotonically with the strengthening of e–ph coupling $\alpha$, but a decrease occurs in the range of $2.24 < \alpha < 2.45$ eV Å$^{-1}$ in the present calculation. The reason is not clear. It is possibly due to the fact that the bipolaron contains two electrons (or holes). With increasing e–ph coupling strength, an oscillation might take place for some localized states with double-peak characteristics, such as c1 and v1 (see figure 7). At stronger e–ph coupling ($\alpha > 2.4$ eV Å$^{-1}$), another two new shallow energy levels, designated c2 and v2, emerge from the bottom of the conduction band and the top of the lowest sub-valence band separately.

The effect of e–e interactions on the localized levels was studied by considering the Hubbard term $U$ in PtCl. It was found that the energy bands together with the localized levels will move up. In the soliton or bipolaron case, e–e interaction will enlarge the mini-gap between v1 (v2) and the VB, that is the e–e interaction will deepen the shallow level v1 (v2).

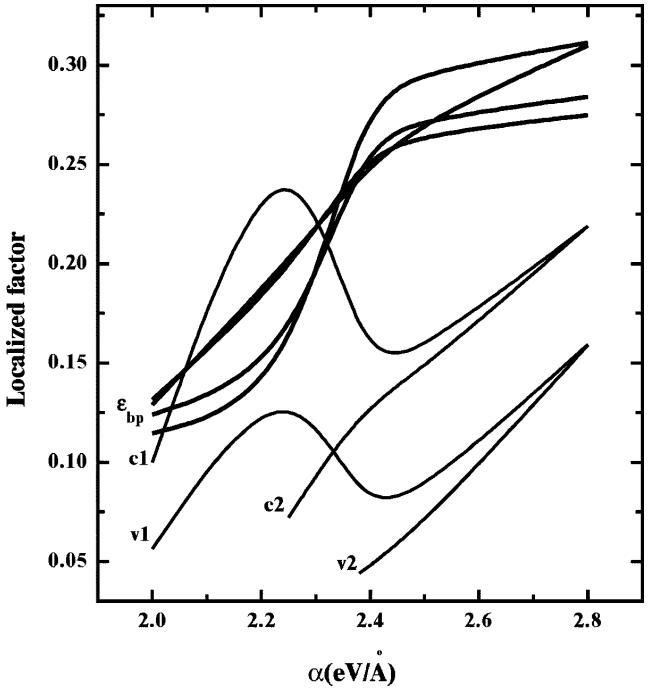


**Figure 7.** Dependence of the localization factors of the shallow and deep energy levels of a bipolaron on the e–ph coupling constant $\alpha$ in PtCl. The wide lines represent the deep levels and the narrow lines the shallow ones.

The localization of the wavefunction of v1 (v2) will increase due to the e–e interaction. But for c1and c2, the situation is the opposite. For example, in the soliton case, at $U = 0.5t_0$ the mini-gap between c1 (c2) and CB decreases to 0.03 eV (0.005 eV) from 0.05 eV (0.03 eV) of the non-e–e-interaction case. Level c2 will merge into the conduction band when $U > 0.6t_0$, and the corresponding wavefunction will become extended. Similar results were obtained in PtBr compounds.

## 4. Conclusion

In the framework of the two-band tight-binding model, some new shallow levels were found in the forbidden bands in addition to the deep levels of solitons and bipolarons. These shallow levels are situated at the band edges of the CB and the lowest VB. The electronic states of the shallow levels are localized around the excitations. It is expected that these shallow levels will be observed in the absorption spectrum of MX compounds. In addition e–e interactions will decrease the mini-gap between the shallow levels and CB and increase the mini-gap between the shallow levels and VB.

## Acknowledgments

This work was supported by the National Natural Science Foundation, grant No 59871024, and the Foundation of the Ministry of Education for Excellent Returnees.

## References


[1] Baeriswyl D and Bishop A R 1988 *J. Phys. C: Solid State Phys.* **21** 339
[2] Degiorgi L, Wachter P, Haruki M and Kurita S 1989 *Phys. Rev.* B **40** 3285
[3] Okamoto H, Toriumi K, Mitami T and Yamashita M 1989 *Phys. Rev.* B **42** 10 381
[4] Wangbo M H and Foshee M J 1981 *Inorg. Chem.* **20** 113
[5] Toriumi K, Wada Y, Mitani T, Bandow S, Yamashita M and Fujii Y 1989 *J. Am. Chem. Soc.* **111** 2341
[6] Tanino H, Syassen K and Takahashi K 1989 *Phys. Rev.* B **39** 3125
[7] Donohoe R J, Ekberg S A, Tait C D and Swanson B I 1989 *Solid State Commun.* **71** 49
[8] Long F H, Love S P, Swanson B I and McKenzie R H 1993 *Phys. Rev. Lett.* **71** 762
[9] Kanner G S, Gammel J T, Love S P, Johnson S R, Scott B and Swanson B I 1994 *Phys. Rev.* B **50** 18 682
[10] Okamoto H, Mitani T, Toriumi K and Yamashita M 1992 *Phys. Rev. Lett.* **69** 2248
[11] Okamoto H *et al* 1994 *Mol. Cryst. Liq. Cryst.* **256** 161
[12] Okamoto H *et al* 1996 *Phys. Rev.* B **54** 8438
[13] Gammel J T, Saxena A, Batistić I, Bishop A R and Phillpot S R 1992 *Phys. Rev.* B **45** 6408
[14] Weber-Milbrodt S M, Gammel J T, Bishop A R and Loh E Y Jr 1992 *Phys. Rev.* B **45** 6435
[15] Sun X, Yu Z G, Lee K H, Park T Y and Lin D L 1995 *Synth. Met.* **70** 1199
[16] Huang Q F, Wu C Q and Sun X 1995 *Phys. Rev.* B **52** 5637
[17] Matsushita E 1995 *Phys. Rev.* B **51** 17 332
[18] Iwano K 1997 *J. Phys. Soc. Japan* **66** 1088
[19] Wada Y, Mitani T, Yamashita M and Koda T 1989 *J. Phys. Soc. Japan* **58** 3013
[20] Fu Rouli, Xie Shijie, Wu Changqin and Sun Xin 1987 *Chin. Phys. Lett.* **4** 350
[21] Sun Xin, Lu Ding wei, Fu Rouli, Li X S, Lin D L and George T F 1989 *Phys. Rev.* B **40** 12 446
[22] Albers R C 1989 *Synth. Met.* **29** F169
Alouani M, Albers C, Wills J M and Springborg M 1992 *Phys. Rev. Lett.* **69** 3104
[23] Painelli A and Grilando A 1989 *Phys. Rev.* B **39** 9663
Painelli A and Grilando A 1989 *Synth. Met.* **29** F181
[24] In the several contributions on MX chains in the proceedings of the *International Conference on the Science and Technology of Synthetic Metals, ICSM 1990 (Tübingen, 1990) Synth. Met.* **41–43** (1991)
[25] Gammel J T, Donohoe R J, Bishop A R and Swanson B I 1990 *Phys. Rev.* B **42** 10 566
[26] Kurita S, Haruki M and Miyagawa K 1988 *J. Phys. Soc. Japan* **57** 1789
[27] Donohoe R J, Ekberg S A, Tait C D and Swanson B I 1989 *Solid State Commun.* **71** 49
[28] Donohoe R J, Worl L A, Arrington C A, Bulou A and Swanson B I 1992 *Phys. Rev.* B **45** 13 185
[29] Okamoto H *et al* 1992 *Mol. Cryst. Liq. Cryst.* **218** 247
[30] Xie Shi-Jie, Wei Jian-Hua, Mei Liang-Mo, Han Sheng-Hao and Lai Shu-Shen 1998 *J. Phys. C: Solid State Phys.* **10** 2291